

MTGAT: Multimodal Temporal Graph Attention Networks for Unaligned Human Multimodal Language Sequences

Jianing Yang^{*1}, Yongxin Wang^{*1}, Ruitao Yi¹, Yuying Zhu¹, Azaan Rehman¹,
Amir Zadeh¹, Soujanya Poria², Louis-Philippe Morency¹

¹ Carnegie Mellon University, ² Singapore University of Technology and Design
{jianing3, yongxinw, ruitaoy, yuyingz, arehman, abagherz}@cs.cmu.edu, sporia@sutd.edu.sg, morency@cs.cmu.edu

Abstract

Human communication is multimodal in nature; it is through multiple modalities, i.e., language, voice, and facial expressions, that opinions and emotions are expressed. Data in this domain exhibits complex multi-relational and temporal interactions. Learning from this data is a fundamentally challenging research problem. In this paper, we propose Multimodal Temporal Graph Attention Networks (MTGAT). MTGAT is an interpretable graph-based neural model that provides a suitable framework for analyzing this type of multimodal sequential data. We first introduce a procedure to convert unaligned multimodal sequence data into a graph with heterogeneous nodes and edges that captures the rich interactions between different modalities through time. Then, a novel graph operation, called Multimodal Temporal Graph Attention, along with a dynamic pruning and read-out technique is designed to efficiently process this multimodal temporal graph. By learning to focus only on the important interactions within the graph, our MTGAT is able to achieve state-of-the-art performance on multimodal sentiment analysis and emotion recognition benchmarks including IEMOCAP and CMU-MOSI, while utilizing significantly fewer computations.

1 Introduction

With recent advances in machine learning research, analysis of multimodal sequential data has become an increasingly prominent research area. At the core of modeling this form of data, there are the fundamental research challenges of *fusion* and *alignment*. Fusion is the process of blending information from multiple modalities. It is usually preceded by alignment, which is the process of finding temporal relations between the modalities. An important research area that exhibits this form of data is multimodal language analysis, where sequential modalities of language, vision, and acoustic are present. These three modalities carry the communicative information and interact with each other through time; e.g. positive word at the beginning of an utterance may be the cause of a smile at the end. In analyzing such multimodal sequential data, it is crucial to utilize a model that is capable of performing both fusion and alignment accurately and efficiently by a) aligning arbitrarily distributed asynchronous modalities in an interpretable manner, b) efficiently accounting for short and long-range dependencies, c) explicitly modeling

the intermodal interactions between the modalities while simultaneously accounting for intra-model dynamics. To this end, we introduce MTGAT (Multimodal Temporal Graph Attention Networks). MTGAT is a flexible, parameter-efficient and interpretable graph-based neural model that extends the Graph Attention Networks (GAT) (Veličković et al. 2018) to learn fusion and alignment of asynchronous multimodal sequence data. For MTGAT, the modalities do not need to be pre-aligned and they do not need to follow the same sampling rate (as required by previous models (Chen et al. 2017)). In this paper, we show that MTGAT, with the help of a novel graph pruning method, yields a parameter-efficient tool for multimodal sequential learning. Comprehensive experiments on two multimodal emotion recognition and sentiment analysis benchmarks, IEMOCAP and CMU-MOSI, show on-par (and sometimes superior) performance with state-of-the-art methods while requiring only a fraction of previous method’s model parameters. In visualizing the edges of the MTGAT, we observe successful fusion and alignment of trimodal data.

2 Related Works

Human Multimodal Language Analysis Analyzing human multimodal language involves learning from data across multiple heterogeneous sources of information, i.e. language, visual, and acoustic modalities. Instead of learning representations from a single modality, Lazaridou, Pham, and Baroni (2015) fused language and visual information by extending the skip-gram model. Similarly, Ngiam et al. (2011) fused visual and acoustic knowledge using deep learning networks. More recently, other methods for learning multimodal representations have been proposed. A hierarchical multimodal architecture with attention and word-level fusion is proposed for sentiment analysis and emotion recognition (Gu et al. 2018). Another model that combines deep canonical correlation analysis with cross-modal autoencoders is put forward for multimodal sentiment classification task (Dumpala et al. 2019). Pham et al. (2019) learned joint multimodal representations through cyclic modality translations. These earlier approaches made the assumption that the multimodal sequences they receive are aligned based on word boundaries. To date, modeling unaligned multimodal language sequences remains understudied in deep learning, except for Tsai et al. (2019a), who proposed to use cross-modal Transformers to model unaligned multimodal language sequences. However, a cross-

^{*}Equal contribution

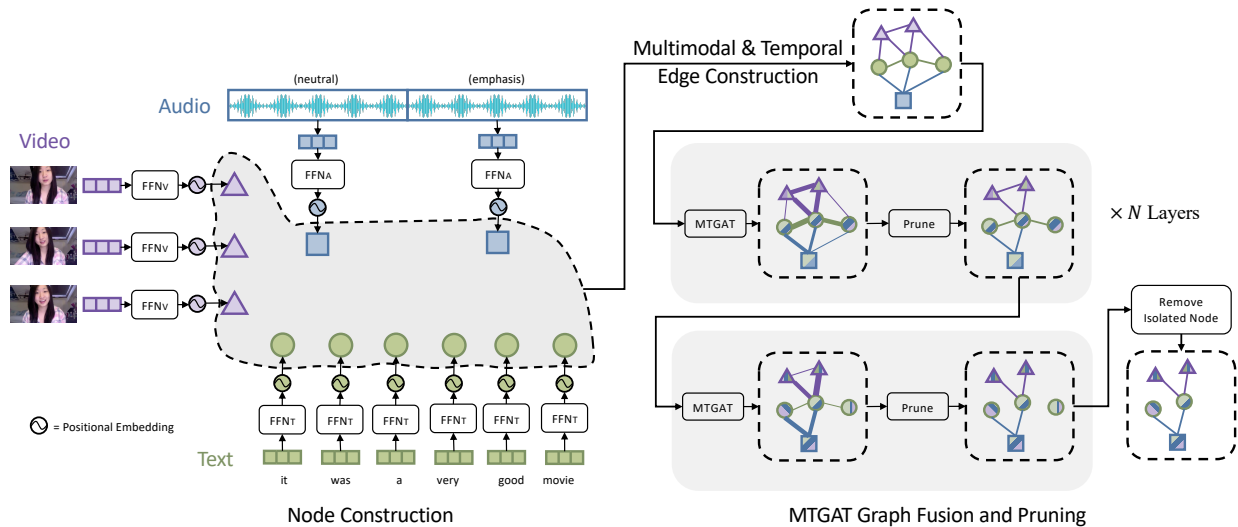


Figure 1: The 3-stage MTGAT framework: Node Construction, Edge Construction and Fusion+Pruning. **[Node Construction]** Each modality’s features are first passed through a distinct Feed-Forward-Network to be mapped into the same embedding size. Then, a positional embedding is added to each transformed feature based on its position in its own modality, so that temporal information are encoded. The features are now nodes in the graph. **[Edge Construction]** We then apply an algorithm to construct edges among these nodes by appropriately indexing each edge with a modality type and a temporal type. **[Fusion+Pruning]** Finally, we pass the graph into the MTGAT module to learn interactions across modality and time. The output graph with updated node embeddings and pruned edges can be passed to downstream modules, e.g. a Multi-layer Perceptron, to complete specific tasks such as regression or classification.

modal Transformer module is a bi-modal module which can only account for two modalities’ input at a time. As a result, Tsai et al. (2019a) uses multiple cross-modal Transformers and applies late fusion to obtain tri-modal features, resulting in a large amount of parameters needed to retain original modality information. In contrast, our proposed graph method, with very small amount of model parameters, can aggregate information from multiple (more than 2) modalities at early stage by simply having an edge between the corresponding modalities, allowing richer and more complex representation of the interactions to be learned.

Graph Neural Networks Graph Neural Networks (GNNs) were introduced in (Gori, Monfardini, and Scarselli 2005; Scarselli et al. 2008) with an attempt to extend deep neural networks to handle graph-structured data. Since then, there has been an increasing research interest on generalizing deep neural network’s operations such as convolution (Kipf and Welling 2016; Schlichtkrull et al. 2017; Hamilton, Ying, and Leskovec 2017), recurrence (Nicolicioiu, Duta, and Leordeanu 2019), and attention (Veličković et al. 2018) to graph. The most relevant work to this paper is (Veličković et al. 2018), where Graph Attention Networks (GAT) was proposed. GAT is the first graph convolution that incorporates the attention mechanism when aggregating nodes.

Recently, more heterogeneous GNN methods (Wang et al. 2019a; Wei et al. 2019; Shi et al. 2016) have been proposed. These methods assume the nodes represent heterogeneous data. The heterogeneous nodes referred in these works consist of different data entities, as opposed to different views

of the same data entity. In the NLP domain, we have seen multimodal GNN methods (Khademi 2020; Yin et al. 2020) being proposed for different view of the same data entity, on tasks such as Visual Question Answering and Machine Translation. However, these multimodal data still differs from our setting because they are mostly static pictures and short text which does not have a temporal nature like video data.

To the best of our knowledge, there has been little research on modeling human multimodal language data, which includes video, audio and text, with graph-based method. In this paper, we demonstrate the effectiveness of modelling such data with the proposed MTGAT graph-based method.

3 Model

In this section, we describe our proposed framework: Multimodal Temporal Graph Attention Networks (MTGAT) for unaligned multimodal language sequences. Figure 1 gives a high-level overview of the framework. For clarity, we describe the framework in three stages: Node Construction, Edge Construction and Fusion+Pruning.

3.1 Node Construction

Our goal is to define a graph with multimodal nodes. As illustrated in Figure 1, each modality’s input feature vector is passed through a modality-specific Feed-Forward-Network (FFN). This allows input from each modality to be transformed into the same embedding size. A positional embedding is then added (separately for each modality) to each embedding to encode temporal information. The output of this operation becomes a node in the graph. Each node is

marked with a modality identifier π , where

$$\pi \in \{\text{Audio, Video, Text}\}$$

This modality identifier will be used later at the fusion stage.

Positional Embeddings Because graph neural network has no recurrence, we need to inject positional information into each node. For this purpose, we add a positional embedding to each node’s feature vector prior to being used as input to the graph. Positional information is based on the node’s position in the sequence. The specific implementation is similar to those used in Transformer models (Vaswani et al. 2017), where a fixed, interleaving sine and cosine embedding is used:

$$PE_{(pos, 2i)} = \sin(pos/10000^{2i/d_{emb}})$$

$$PE_{(pos, 2i+1)} = \cos(pos/10000^{2i/d_{emb}})$$

3.2 Edge Construction

In this section we outline how the edges of the graph are constructed.

Fully Connected Graph with Edge Type We make no assumption about prior alignment of the modalities, thus the model needs to learn to align. To this end, we construct an initially fully connected graph so that the model is free to search the space of possible alignments. It is worth noting that the edges in the graph are *directed*, because, as we will see later in the fusion stage, the attention operation we use is asymmetric; thus imposing a different semantic for edge (i, j) than edge (j, i) . We construct multimodal edges by labeling each edge with a modality type identifier ϕ , where

$$\phi \in \{A-A, A-V, A-T, V-A, V-V, V-T, T-A, T-V, T-T\}$$

The A-T notation here denotes the modality type of the source node (A) and the modality type of the target node (T). A is short for Audio, V is short for Video and T is short for Text. As we will see, this edge modality identifier ϕ will be used later in the Multimodal Temporal Graph Attention mechanism to select which attention vector should be used for a specific edge.

Pseudo-alignment and Temporal Edges For video emotion and sentiment analysis, the order of the sequence elements plays a key role (Poria et al. 2017). For example, a transition from a frown to a smile ($\ominus \rightarrow \odot \rightarrow \odot$) may imply a positive sentiment, where as a transition from a smile to a frown ($\odot \rightarrow \ominus \rightarrow \ominus$) may imply a negative sentiment. For this reason, in addition to the modality type we defined earlier, we also define a temporal type for each edge as follows:

$$\tau \in \{\text{past, present, future}\}$$

Specifically, we mark edges incident from nodes in the past (source node happens earlier in time than target node) with edge temporal identifier “past”; we mark the edges incident from nodes in the future (source node happens later in time than target node) with edge temporal identifier “future”¹;

¹Note, in online cases where future information is not available these edges can be removed.

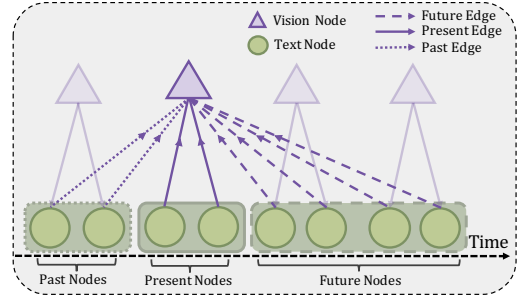


Figure 2: An example of the pseudo-alignment between two unaligned sequences. We treat the vision nodes as “buckets” and fit the longer text sequence into the vision “buckets”.

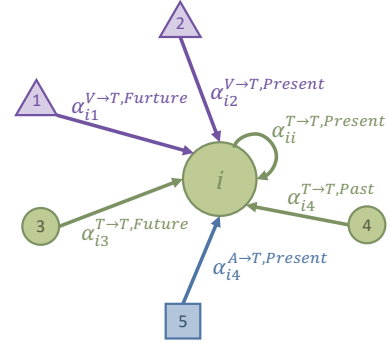


Figure 3: A closer look at the MTGAT operation.

all other edges are marked with “present”. Within a single modality, determining a past, present or future edge can be easily done by comparing the positions of the nodes that it connects. However, there is no definition of “earlier” or “later” between nodes from two different modalities, due to the unaligned nature of our input sequences. To this end, we introduce the pseudo-alignment heuristic that coarsely defines the past, present and future connections between nodes across two modalities. Given a node from one modality, our pseudo-alignment heuristic first determines a set of nodes in the other modality that should be considered as “present” with respect to the given node. All nodes in the other modality that exists after this set of “present” nodes are considered “future” nodes, and all those before are considered “past” nodes. Then similar to the unimodal scenario, incident edges from the “future” nodes are marked as “future”, and all those from the “past” are marked as “past”.

In order to determine the set of “present” nodes for the given node, we treat one modality as “buckets” and try to distribute along time the nodes in the other modality into each of the “buckets” as *evenly* as possible. Figure 2 shows an example of our pseudo-alignment. For more details, please refer to the Appendix.

3.3 Fusion and Pruning

Multimodal Temporal Graph Attention With our formulation of the graph, we need a new operation that can model the multimodal nature of the nodes and the temporal nature

Algorithm 1: MTGAT with edge pruning

Input : $\mathcal{G}(\mathcal{V}, \mathcal{E})$: The multimodal graph,
 \mathbf{x}_i : The center node's feature,
 $\mathbf{x}_j, \forall j \in \mathcal{N}_i$: The neighbor node's feature,
 π_i : Node type of node i 's,
 τ_{ij} : Temporal type of the edge (j, i) ,
 ϕ_{ij} : Modality type of the edge (j, i) ,
 H : Number of attention heads,
 k : Prune percentage

Output : \mathbf{z}_i : Node output feature,
 $\mathcal{G}'(\mathcal{V}, \mathcal{E}')$: The updated graph

```
1 Node type specific transformation  $\mathbf{x}'_i \leftarrow \mathbf{M}_{\pi_i} \mathbf{x}_i, \forall i, j$ 
2 for  $h = 1 \dots H$  do
3   for  $j \in \mathcal{N}_i$  do
4     calculate raw attention score using modality-
       and temporal-edge-type specific parameters:
        $\beta_{[h],i,j} = \text{LeakyRelu}(\mathbf{a}_{[h]}^{\phi_{ji}, \tau_{ji}} \cdot [\mathbf{x}'_i \parallel \mathbf{x}'_j])$ 
5   normalize raw attention scores over  $\mathcal{N}_i$  to get
       attention weight  $\alpha_{[h],i,j}$ 
6 calculate node output feature
    $\mathbf{z}_i = \text{concat}(\sum_{h=1}^H \alpha_{[h],i,j} \mathbf{x}'_j)$ 
7 calculate average attention weight across all heads
    $\bar{\alpha}_{i,j} = \frac{1}{H} \sum_{h=1}^H (\alpha_{[h],i,j})$ 
8 sort  $\bar{\alpha}_{i,j}$  and delete the edges with the smallest  $k\%$ 
   average attention weight from  $\mathcal{E}$ , obtaining  $\mathcal{E}'$ 
9 return  $\mathbf{z}_i, \mathcal{G}'(\mathcal{V}, \mathcal{E}')$ 
```

of the edges. We propose Multimodal Temporal Graph Attention (MTGAT) to address these two characteristics. An algorithm of our method is shown in Algorithm 1 and a pictorial illustration is given in Figure 3. Specifically, the first step is to transform all node's features into a common feature space. We use a simple linear transformation:

$$\mathbf{x}'_i = \mathbf{M}_{\pi_i} \mathbf{x}_i,$$
$$\pi_i \in \{\text{Audio, Video, Text}\}$$

Note that this transformation is done based on the node's modality identifier π , to allow each modality's node be transformed differently.

Then, for each neighbor node j that has an edge incident into a center node i , we compute a raw attention score β based on that edge's modality and temporal type:

$$\beta_{i,j} = \text{LeakyRelu}(\mathbf{a}^{\phi_{ji}, \tau_{ji}} \cdot [\mathbf{x}'_i \parallel \mathbf{x}'_j])$$

Note that we learn one attention vector $\mathbf{a}^{\phi, \tau}$ per each edge type. The edge type is determined by a tuple (ϕ, τ) of the edge modality identifier and the edge temporal identifier. Under our 3-modality setting, this results in 27 edge types (9 modality types \times 3 temporal types).

Then we normalize the raw attention scores over all neighbor nodes j with Softmax so that the normalized attention weight sums to 1 to preserve the scale of the node features in the graph.

$$\alpha_{ij} = \frac{\exp(\beta_{i,j})}{\sum_{k \in \mathcal{N}_i} \exp(\beta_{i,k})}$$

Then, node i aggregates information from neighbor nodes by performing a weighted sum over all neighbor's transformed feature, with the attention weight as the coefficient:

$$\mathbf{z}_i = \sum_{j \in \mathcal{N}_i} \alpha_{i,j} \mathbf{x}'_j$$

\mathbf{z}_i now becomes the new node embedding for node i . After aggregation, node i transformed from a unimodal node into a multimodal node (illustrated by the mixing of colors of the nodes in Figure 1) that carries rich information from its neighbor. As described in previous sections, because our graph is a fully connected one, node i can gather information from all modalities at all timestamps, allowing rich and complex cross-modal and temporal interactions to be modeled.

The heterogeneous input data of the multimodal graph could be of different scales, making the variance of the data high. Previous work (Wang et al. 2019b) has shown using multi-head attention, as oppose to single-head attention, could help stabilize the training process. We incorporate this idea into our model by repeating the edge-type specific attention vector H times, where H is a hyperparameter representing the number of attention heads. With multi-head attention, the output node feature \mathbf{z}_i is obtained by concatenating each head's output:

$$\mathbf{z}_i = \text{concat}(\sum_{h=1}^H \alpha_{[h],i,j} \mathbf{x}'_j)$$

Dynamic Edge Pruning Our graph formulation models all-to-all interactions for all 27 edge types. This design results in a very large number of edges in the graph, making the computation graph difficult to fit into GPU memories. More importantly, when there are so many edges, it is hard to avoid some of these edges from inducing spurious correlations and distracting the model from focusing on the truly important interactions (Lee, Lee, and Kang 2019; Knyazev, Taylor, and Amer 2019). It has been shown in these previous work that pruning serves as an effective regularization for graph learning problems. This observation motivates us to use an edge pruning technique to reduce memory consumption and to regularize the model. We propose a simple method: Dynamically prune edges with low attention weight. Specifically, after each layer of MTGAT, we have the attention weight $\alpha_{[h],i,j}$ for each attention head h for each edge (i, j) . We take the average of the attention weights over the attention heads:

$$\bar{\alpha}_{i,j} = \frac{1}{H} \sum_{h=1}^H (\alpha_{[h],i,j})$$

Then, we sort $\bar{\alpha}_{i,j}$ and delete $k\%$ edges with the smallest attention weights, where k is a hyperparameter. These deleted edges will no longer be calculated in the next MTGAT layer. Our ablation study in Section 5.2 empirically verifies the effectiveness of this approach.

3.4 Graph Readout

At the end of the fusion process, we need to read out information scattered in the nodes into a single vector so that we can pass it through a classification head. Recall that the pruning

Model \ Emotion	Happy	Sad	Angry	Neutral
(Word Aligned) IEMOCAP Emotions				
EF-LSTM	84.2	80.5	84.5	67.1
LF-LSTM	86.3	81.7	83.0	67.6
RMFN	85.8	85.1	84.2	69.1
MFM	85.8	86.1	86.7	68.1
MFN	84.0	82.1	83.7	69.2
RAVEN	85.8	83.1	86.7	69.3
MCTN	83.1	79.6	80.4	57.0
MuT	88.6	86.0	87.0	70.7
MTGAT (ours)	88.4	86.1	87.2	72.3
(Unaligned) IEMOCAP Emotions				
CTC + EF-LSTM	75.7	70.5	67.1	57.4
LF-LSTM	71.8	70.4	67.9	56.2
CTC + RAVEN	76.8	65.6	64.1	59.5
CTC + MCTN	77.5	71.7	65.6	49.3
MuT	81.9	74.1	70.2	59.7
MTGAT (ours)	86.0	79.9	76.7	64.1

Table 1: F1 Scores on IEMOCAP. \uparrow means higher is better and \downarrow means lower is better.

process drops edges in the graph. If all edges incident into a node have been dropped, then it means that node was not updated based on its neighbors. In that case, we simply ignore that node in the readout process.

$$\mathcal{V}' = \{\mathcal{V} \mid \mathcal{V} \in \mathcal{V} \text{ and } \text{count_incident_edge}(\mathcal{V}) > 0\}$$

For CMU-MOSI and IEMOCAP, we readout the graph by averaging all the surviving node’s output features into one vector. This vector is then passed to a Multi-Layer-Perceptron (MLP) to make a prediction.

4 Experiments

We empirically evaluate MTGAT model on two datasets: IEMOCAP (Busso et al. 2008) and CMU-MOSI (Zadeh et al. 2016); both are well-known datasets used by prior works (Liang et al. 2018; Pham et al. 2019; Tsai et al. 2019b,a) to benchmark multimodal emotion recognition and sentiment analysis.

4.1 Dataset and Metrics

IEMOCAP IEMOCAP is a multimodal emotion recognition dataset consisting of 10K videos. The task we chose is the 4-way multilabel emotion classification, classifying into happy, sad, angry and neutral. For train split, the positive/negative label ratio for each emotion is 954:1763, 338:2379, 690:2027 and 735:1982. For the test split, the ratio is 383:555, 135:803, 193:745 and 227:711. Due to this unbalanced distribution of the the labels, we use F1 score as a better metric for comparison.

Metric	Acc ₇ \uparrow	Acc ₂ \uparrow	F1 \uparrow	MAE \downarrow	Corr \uparrow
(Word Aligned) CMU-MOSI Sentiment					
EF-LSTM	33.7	75.3	75.2	1.023	0.608
LF-LSTM	35.3	76.8	76.7	1.015	0.625
RMFN	38.3	78.4	78.0	0.922	0.681
MFM	36.2	78.1	78.1	0.951	0.662
MFN	34.1	77.4	77.3	0.965	0.632
RAVEN	33.2	78.0	76.6	0.915	0.691
MCTN	35.6	79.3	79.1	0.909	0.676
MuT	40.0	83.0	82.8	0.871	0.698
MTGAT (ours)	39.1	81.9	81.7	0.881	0.709
(Unaligned) CMU-MOSI Sentiment					
CTC+EF-LSTM	31.0	73.6	74.5	1.078	0.542
LF-LSTM	33.7	77.6	77.8	0.988	0.624
CTC+MCTN	32.7	75.9	76.4	0.991	0.613
CTC+RAVEN	31.7	72.7	73.1	1.076	0.544
MuT	39.1	81.1	81.0	0.889	0.686
MTGAT (ours)	37.2	81.5	81.5	0.887	0.701

Table 2: Results on CMU-MOSI.

Model	# Parameters
MuT (previous SOTA)	2.24 M
MTGAT (ours)	0.14 M

Table 3: Number of model parameters (in Millions).

CMU-MOSI CMU Multimodal Opinion Sentiment Intensity is a multimodal sentiment analysis dataset with 2,199 movie review video clips. Each video clip is labeled with real-valued sentiment score within $[-3, +3]$, with 3 being a very positive sentiment and -3 a very negative one. Following previous works (Tsai et al. 2019a), we report five metrics: 7-class classification accuracy (Acc₇), binary classification accuracy (Acc₂, positive/negative sentiments), F1 score, Mean Absolute Error (MAE) and the correlation of the model’s prediction with human.

We follow prior works (Tsai et al. 2019a) to evaluate on two versions of each dataset: a word-aligned version and an unaligned version.

4.2 Baselines

For both aligned and unaligned evaluations, we use Early Fusion LSTM (EF-LSTM) and Late Fusion LSTM (LF-LSTM) (Tsai et al. 2019a) as baselines. For the aligned benchmarks alone, we additionally compare to Recurrent Attended Variation Embedding Network (RAVEN) (Wang et al. 2019c), Recurrent Multistage Fusion Network (RMFN) (Liang et al. 2018), MFM (Tsai et al. 2019b), Memory Fusion Network (MFN) (Zadeh et al. 2018) and Multimodal Cyclic Translation Network (MCTN) (Pham et al. 2019). For the un-aligned benchmarks, we compare our model against similar methods

as in previous works (Tsai et al. 2019a), which combine a Connectionist Temporal Classification (CTC) loss (Graves et al. 2006) with the pre-existing methods such as EF-LSTM, MCTN, RAVEN.

4.3 Results

Shown in Table 1 and Table 2, our model, MTGAT, outperforms previous methods on aligned/unaligned IEMO-CAP benchmark and unaligned CMU-MOSI benchmark by a large margin. MTGAT also achieves on-par performance on aligned CMU-MOSI with previous state of the art. It is possible that the hard-alignment in aligned CMU-MOSI dataset may have prevented our model from learning the best alignment and fusion for this particular benchmark, thus resulting in suboptimal performance. Overall, with an extremely small number of parameters, our model is able to learn better alignment and fusion for multimodal sentiment analysis task. Details regarding our model and hyper-parameters can be found in the Appendix.

Parameter Efficiency (MTGAT vs MulT) We discover that MTGAT is a highly parameter-efficient model. A comparison of model parameters between MTGAT and MulT (Tsai et al. 2019a) (previous state of the art) is shown in Table 3. The hyperparameter used for this comparison can be found in the Appendix. With only a fraction (6.25%) of MulT’s parameters, MTGAT is able to achieve on-par, and in many cases superior performance on the two datasets. This demonstrates the parameter efficiency of our method.

Qualitative Analysis The attention weights on the graph edges forms a natural way to interpret our model. We visualize the edges to probe what MTGAT has learned. The following case study is a randomly selected video clip from the CMU-MOSI validation set. We observe the phenomena shown below is a general trend.

In Figure 4, we show an example of the asymmetric bi-modal relations between vision and text. We observe that our model picks on meaningful relations between words such as “**I really enjoyed**” and facial expressions such as raising eyebrow, highlighted in the red dashed boxes in Figure 4a. Our model can also learn long-range correlation between “**I really enjoy**” and head nodding. Interestingly, we discover that strong relations that are not detected by vision-to-text edges can be recovered by the text-to-vision edges. This advocates the design of the multi-type edges, which allows the model to learn different relations independently that can complement one another.

Figure 5 gives a holistic view of the attention weights among all three modalities. We observe a pattern where almost all edges involve the text modality. A possible explanation for this observation is that the text is the dominant modality with respect to the sentiment analysis task. This hypothesis is verified by the ablation study in Sec. 5.3. Meanwhile, there appears to be very small amount of edges connecting directly between vision and audio, indicating that there might be little meaningful correlation between them. This resonates with our ablation studies in Table 4, where

Ablation	Acc ₂ ↑	F1 ↑	MAE ↓
Edge Types			
No Edge Types	82.4	82.5	0.937
Multimodal Edges Only	85.6	85.7	0.859
Temporal Edges Only	85.2	85.2	0.887
Pruning			
Random Pruning Keep 80%	75.5	74.5	1.080
No Pruning	84.7	84.7	0.908
Modalities			
Language Only	81.5	81.4	0.911
Vision Only	57.0	57.1	1.41
Audio Only	58.1	58.1	1.37
Vision, Audio	62.0	59.2	1.360
Language, Audio	82.4	82.5	0.942
Language, Vision	86.6	86.6	0.865
Full Model, All Modalities	86.6	86.6	0.861

Table 4: Ablation on un-aligned CMU-MOSI validation set.

vision and audio combined produce the lowest bi-modal performance. Under such circumstance, our MTGAT learns to kill direct audio-vision relations and instead fuse their information indirectly using the text modality as a proxy, whereas previous methods such as MulT keeps audio-vision attentions alive along the way, introducing possible spurious relations that could distract model learning.

5 Ablation Study

We conduct ablation study using unaligned CMU-MOSI dataset. MTGAT Full Model implements multimodal temporal edge types, adopts TopK edge pruning that keeps edges with top 80% edge weights, and includes all three modalities as its input. Table 4 shows the performance. We present research questions (RQs) as follows and discuss how ablation studies address them.

5.1 RQ1: Does using 27 edge types help?

We first study the effect of edge types on our model performance. As we incrementally add in multimodal and temporal edge types, our model’s performance continues to increase. The model with 27 edge types performs the best under all metrics. By dedicating one attention vector $\mathbf{a}^{\phi, \tau}$ to each type of edges, MTGAT can model each complex relation individually, without having one relation interfering another. As shown in Figure 4 and Table 4, such design enhances multimodal fusion and alignment, helps maintain long-range dependencies in multimodal sequences, and yields better results.

5.2 RQ2: Does our pruning method help?

We compare our TopK edge pruning to no pruning and random pruning to demonstrates its effectiveness. We find that TopK pruning exceeds both no pruning and random pruning models in every aspect. It is clear that, by selectively keeping

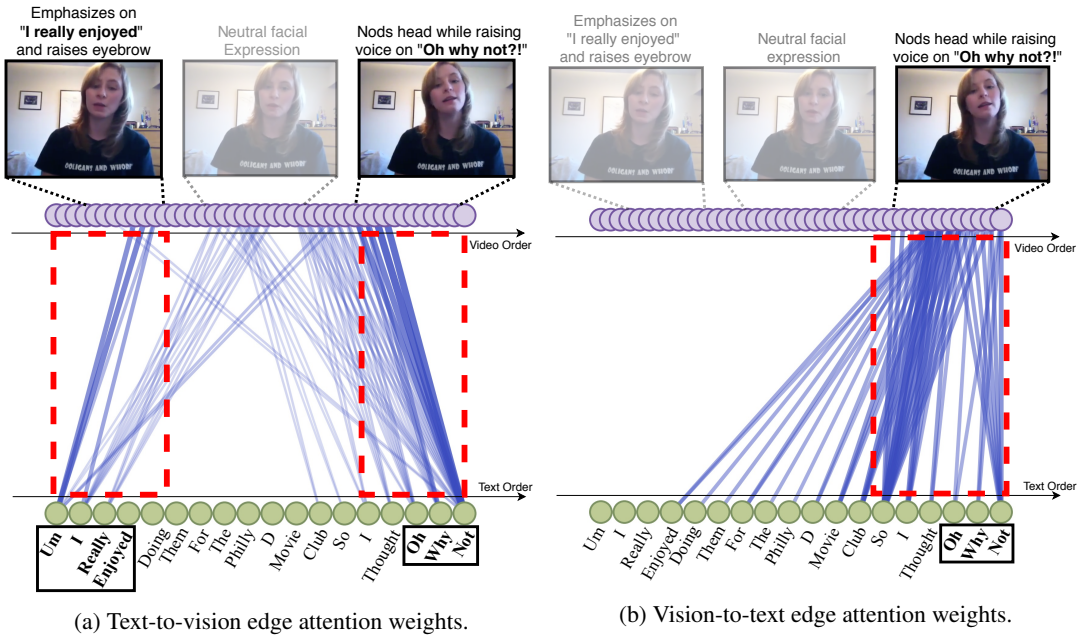


Figure 4: We visualized the asymmetric attention weights of the text-to-vision and vision-to-text edges for one of the validation sequence in CMU-MOSI dataset. The visualized attention weights are from layer 3 of MTGAT. Note that the edge types are not shown here for visual clarity.

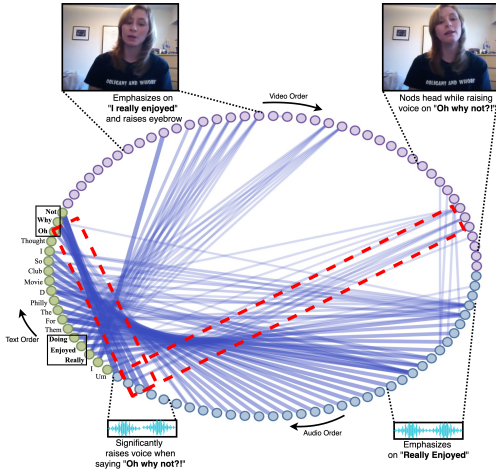


Figure 5: Visualization of tri-modal attention weights.

the top 80% most important edges, our model learns more meaningful representations than randomly keeping 80%. Our model also beats the one where no pruning is applied, which attests to our assumption and observation from previous work (Lee, Lee, and Kang 2019; Knyazev, Taylor, and Amer 2019) that spurious correlations do exist and can distract model from focusing on important interactions. Therefore, by pruning away the spurious relations, the model learned a better representation of the interactions, while using significantly fewer computation resources.

5.3 RQ3: Are all modalities helpful?

Lastly, we study the impact of different modality combinations used in our model. As shown in Table 4, we find that adding a modality consistently brings performance gains to our model. Through the addition of individual modalities, we find that adding the text modality gives the most significant performance gain, indicating that text may be the most dominant modality for our task. This can also be qualitative confirmed by seeing the concentrated edge weights around text modality in Figure 5. This observation also conforms with the observations seen in prior works (Tsai et al. 2019a; Pham et al. 2019). On the contrary, adding audio only brings marginal performance gain. Overall, this ablation study demonstrates that all modalities are beneficial for our model to learn better multimodal representations.

6 Conclusion

In this paper, we presented the Multimodal Temporal Graph Attention Networks (MTGAT). We showed that MTGAT is an interpretable model that is capable of both fusion and alignment. It achieves similar to SOTA performance on two publicly available datasets for emotion recognition and sentiment analysis while utilizing substantially lower number of parameters than a transformer-based model such as MuT.

7 Acknowledgments

This material is based upon work partially supported by BMW of North America, the National Science Foundation and National Institutes of Health. Any opinions, findings, and conclusions or recommendations expressed in this material

are those of the authors and do not necessarily reflect the views of BMW of North America, National Science Foundation or National Institutes of Health, and no official endorsement should be inferred.

References

- Busso, C.; Bulut, M.; Lee, C.-C.; Kazemzadeh, A.; Mower, E.; Kim, S.; Chang, J. N.; Lee, S.; and Narayanan, S. S. 2008. IEMOCAP: Interactive emotional dyadic motion capture database. *Language resources and evaluation* 42(4): 335.
- Chen, M.; Wang, S.; Liang, P. P.; Baltrušaitis, T.; Zadeh, A.; and Morency, L.-P. 2017. Multimodal sentiment analysis with word-level fusion and reinforcement learning. In *Proceedings of the 19th ACM International Conference on Multimodal Interaction*, 163–171.
- Degottex, G.; Kane, J.; Drugman, T.; Raitio, T.; and Scherer, S. 2014. COVAREP—A collaborative voice analysis repository for speech technologies. In *2014 IEEE International Conference on Acoustics, Speech and Signal Processing (ICASSP)*, 960–964. IEEE.
- Dumpala, S. H.; Sheikh, I.; Chakraborty, R.; and Kopparapu, S. K. 2019. Audio-visual fusion for sentiment classification using cross-modal autoencoder. In *Proc. Neural Inf. Process. Syst. (NIPS)*, 1–4.
- Gori, M.; Monfardini, G.; and Scarselli, F. 2005. A new model for learning in graph domains. In *Proceedings. 2005 IEEE International Joint Conference on Neural Networks, 2005.*, volume 2, 729–734. IEEE.
- Graves, A.; Fernández, S.; Gomez, F.; and Schmidhuber, J. 2006. Connectionist temporal classification: labelling unsegmented sequence data with recurrent neural networks. In *Proceedings of the 23rd international conference on Machine learning*, 369–376.
- Gu, Y.; Yang, K.; Fu, S.; Chen, S.; Li, X.; and Marsic, I. 2018. Multimodal Affective Analysis Using Hierarchical Attention Strategy with Word-Level Alignment. In *Proceedings of the 56th Annual Meeting of the Association for Computational Linguistics (Volume 1: Long Papers)*, 2225–2235. Melbourne, Australia: Association for Computational Linguistics. doi:10.18653/v1/P18-1207. URL <https://www.aclweb.org/anthology/P18-1207>.
- Hamilton, W.; Ying, Z.; and Leskovec, J. 2017. Inductive representation learning on large graphs. In *Advances in neural information processing systems*, 1024–1034.
- iMotions. 2017. Facial expression analysis.
- Khademi, M. 2020. Multimodal Neural Graph Memory Networks for Visual Question Answering. In *Proceedings of the 58th Annual Meeting of the Association for Computational Linguistics*, 7177–7188. Online: Association for Computational Linguistics. doi:10.18653/v1/2020.acl-main.643. URL <https://www.aclweb.org/anthology/2020.acl-main.643>.
- Kipf, T. N.; and Welling, M. 2016. Semi-supervised classification with graph convolutional networks. *arXiv preprint arXiv:1609.02907*.
- Knyazev, B.; Taylor, G. W.; and Amer, M. 2019. Understanding attention and generalization in graph neural networks. In *Advances in Neural Information Processing Systems*, 4202–4212.
- Lazaridou, A.; Pham, N. T.; and Baroni, M. 2015. Combining language and vision with a multimodal skip-gram model. *arXiv preprint arXiv:1501.02598*.
- Lee, J.; Lee, I.; and Kang, J. 2019. Self-Attention Graph Pooling. In *ICML*.
- Liang, P. P.; Liu, Z.; Zadeh, A.; and Morency, L.-P. 2018. Multimodal language analysis with recurrent multistage fusion. *arXiv preprint arXiv:1808.03920*.
- Ngiam, J.; Khosla, A.; Kim, M.; Nam, J.; Lee, H.; and Ng, A. Y. 2011. Multimodal deep learning. In *ICML*.
- Nicolicioiu, A.; Duta, I.; and Leordeanu, M. 2019. Recurrent Space-time Graph Neural Networks. In *Advances in Neural Information Processing Systems*, 12838–12850.
- Pennington, J.; Socher, R.; and Manning, C. D. 2014. Glove: Global vectors for word representation. In *Proceedings of the 2014 conference on empirical methods in natural language processing (EMNLP)*, 1532–1543.
- Pham, H.; Liang, P. P.; Manzini, T.; Morency, L.-P.; and Póczos, B. 2019. Found in translation: Learning robust joint representations by cyclic translations between modalities. In *Proceedings of the AAAI Conference on Artificial Intelligence*, volume 33, 6892–6899.
- Poria, S.; Cambria, E.; Hazarika, D.; Majumder, N.; Zadeh, A.; and Morency, L.-P. 2017. Context-Dependent Sentiment Analysis in User-Generated Videos. In *Proceedings of the 55th Annual Meeting of the Association for Computational Linguistics (Volume 1: Long Papers)*, 873–883. Vancouver, Canada: Association for Computational Linguistics. doi:10.18653/v1/P17-1081. URL <https://www.aclweb.org/anthology/P17-1081>.
- Scarselli, F.; Gori, M.; Tsoi, A. C.; Hagenbuchner, M.; and Monfardini, G. 2008. The graph neural network model. *IEEE Transactions on Neural Networks* 20(1): 61–80.
- Schlichtkrull, M.; Kipf, T. N.; Bloem, P.; Berg, R. v. d.; Titov, I.; and Welling, M. 2017. Modeling Relational Data with Graph Convolutional Networks. *arXiv preprint arXiv:1703.06103*.
- Shi, C.; Li, Y.; Zhang, J.; Sun, Y.; and Philip, S. Y. 2016. A survey of heterogeneous information network analysis. *IEEE Transactions on Knowledge and Data Engineering* 29(1): 17–37.
- Tsai, Y.-H. H.; Bai, S.; Liang, P. P.; Kolter, J. Z.; Morency, L.-P.; and Salakhutdinov, R. 2019a. Multimodal Transformer for Unaligned Multimodal Language Sequences. In *Proceedings of the 57th Annual Meeting of the Association for Computational Linguistics*, 6558–6569. Florence, Italy: Association for Computational Linguistics. doi:10.18653/v1/P19-1656. URL <https://www.aclweb.org/anthology/P19-1656>.
- Tsai, Y.-H. H.; Liang, P. P.; Zadeh, A.; Morency, L.-P.; and Salakhutdinov, R. 2019b. Learning factorized multimodal representations. *ICLR*.

Vaswani, A.; Shazeer, N.; Parmar, N.; Uszkoreit, J.; Jones, L.; Gomez, A. N.; Kaiser, L. u.; and Polosukhin, I. 2017. Attention is All you Need. In Guyon, I.; Luxburg, U. V.; Bengio, S.; Wallach, H.; Fergus, R.; Vishwanathan, S.; and Garnett, R., eds., *Advances in Neural Information Processing Systems 30*, 5998–6008. Curran Associates, Inc. URL <http://papers.nips.cc/paper/7181-attention-is-all-you-need.pdf>.

Veličković, P.; Cucurull, G.; Casanova, A.; Romero, A.; Liò, P.; and Bengio, Y. 2018. Graph Attention Networks. *International Conference on Learning Representations* URL <https://openreview.net/forum?id=rJXMPikCZ>. Accepted as poster.

Wang, X.; Ji, H.; Shi, C.; Wang, B.; Ye, Y.; Cui, P.; and Yu, P. S. 2019a. Heterogeneous Graph Attention Network. In *The World Wide Web Conference on - WWW '19*, 2022–2032. San Francisco, CA, USA: ACM Press. ISBN 978-1-4503-6674-8. doi:10.1145/3308558.3313562. URL <http://dl.acm.org/citation.cfm?doid=3308558.3313562>.

Wang, X.; Ji, H.; Shi, C.; Wang, B.; Ye, Y.; Cui, P.; and Yu, P. S. 2019b. Heterogeneous Graph Attention Network. In *The World Wide Web Conference, WWW '19*, 2022–2032. New York, NY, USA: Association for Computing Machinery. ISBN 9781450366748. doi:10.1145/3308558.3313562. URL <https://doi.org/10.1145/3308558.3313562>.

Wang, Y.; Shen, Y.; Liu, Z.; Liang, P. P.; Zadeh, A.; and Morency, L.-P. 2019c. Words can shift: Dynamically adjusting word representations using nonverbal behaviors. In *Proceedings of the AAAI Conference on Artificial Intelligence*, volume 33, 7216–7223.

Wei, Y.; Wang, X.; Nie, L.; He, X.; Hong, R.; and Chua, T.-S. 2019. MMGCN: Multi-modal Graph Convolution Network for Personalized Recommendation of Micro-video. In *Proceedings of the 27th ACM International Conference on Multimedia*, 1437–1445. Nice France: ACM. ISBN 978-1-4503-6889-6. doi:10.1145/3343031.3351034. URL <https://dl.acm.org/doi/10.1145/3343031.3351034>.

Yin, Y.; Meng, F.; Su, J.; Zhou, C.; Yang, Z.; Zhou, J.; and Luo, J. 2020. A Novel Graph-based Multi-modal Fusion Encoder for Neural Machine Translation. In *Proceedings of the 58th Annual Meeting of the Association for Computational Linguistics*, 3025–3035. Online: Association for Computational Linguistics. doi:10.18653/v1/2020.acl-main.273. URL <https://www.aclweb.org/anthology/2020.acl-main.273>.

Yuan, J.; and Liberman, M. 2008. Speaker identification on the SCOTUS corpus. *Journal of the Acoustical Society of America* 123(5): 3878.

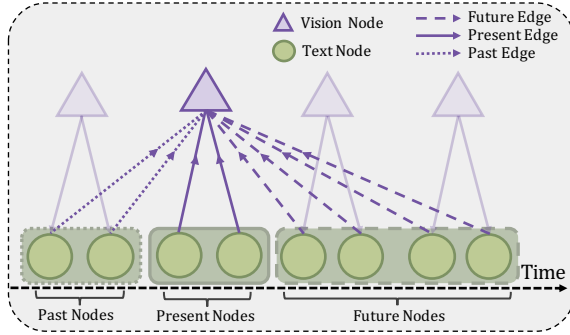
Zadeh, A.; Liang, P. P.; Mazumder, N.; Poria, S.; Cambria, E.; and Morency, L.-P. 2018. Memory fusion network for multi-view sequential learning. *arXiv preprint arXiv:1802.00927*.

Zadeh, A.; Zellers, R.; Pincus, E.; and Morency, L.-P. 2016. Multimodal sentiment intensity analysis in videos: Facial gestures and verbal messages. *IEEE Intelligent Systems* 31(6): 82–88.

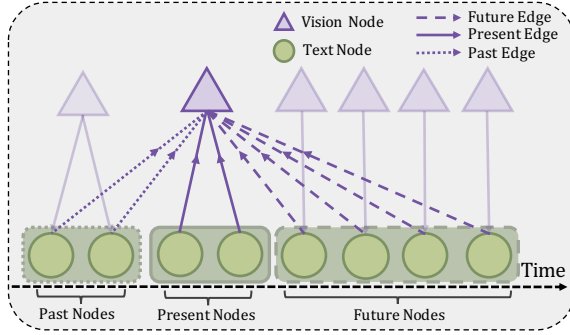
Ethics Statement Building novel algorithms for neural modeling of multimodal language is critical to the success of AI in communication. AI systems needs to understand not just the words but also the subtle nuances of nonverbal communication. Models that are parameter efficient yet as accurate as state of the art, open the door to deployment of accurate deep models to systems with lower computational power. Subsequently, these accurate models of communication can be deployed to cell-phones and embedded systems to assist in building smart technologies; including smart healthcare applications that can better understand emotions and intention, or smart educational platforms that can understand and potentially interpret the students behavioral changes. Therefore, in terms of impact, accurate and efficient models of multimodal language are essential in the future applications of AI.

Appendices

A Details regarding pseudo-alignment



(a) Pseudo-Alignment example with less vision nodes



(b) Pseudo-Alignment example with more vision nodes

Figure 1: More detailed examples of pseudo-align heuristic to coarsely define past, present and future relationships between two unaligned modalities. Again, during pseudo-alignment, we try to spread and match the two modalities as much as uniformly possible (the top figure). When the shorter modality contains more and more nodes, we align as many nodes from the shorter sequence as possible with a minimum window size of 2 to the longer sequence, and the rest nodes from the shorter sequence are aligned with window size of 1 (the bottom figure).

To determine the $\mathcal{V}_{present}$ for v_*^i , we draw an analogy from 1D convolution operation. We are given two sequences of different lengths, and we can treat them as input and output to a 1D convolution operation. Our goal then becomes finding a feasible stride and kernel size that aligns the input, usually the longer sequence, and output, the shorter one. The kernel size that we find defines a group of nodes from the two sequence that should be marked as "present". The stride size here defines how far between each other such groups should spread in time. Without considering padding, we have the following equation in Conv1D operation:

$$\frac{M - W}{S} + 1 = N \quad (1)$$

where M and N are the sequence lengths of the output and input to a Conv1D operator, respectively. W is the kernel size

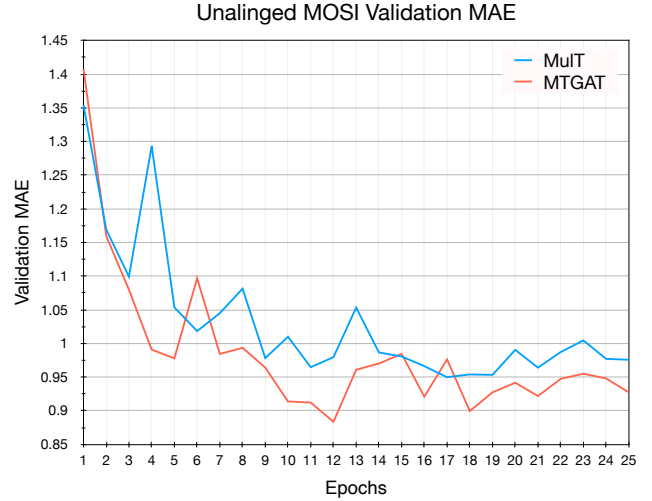


Figure 2: Convergence comparison between MTGAT and MulT on validation set of unaligned MOSI dataset.

and S the stride size. From Eq. 1, we can further write the relationship between W and S as $W = M - (N - 1) * S$. It is clear that the minimum stride size is 1 to a Conv1D operation, and the maximum is $\lfloor \frac{M}{N-1} \rfloor$ in order to keep W positive. We take the average of the minimum and maximum possible values of S as our stride size, so that our kernel size won't be too extreme. In case that $N > \frac{M}{2}$, we set window size as 2 and stride as 2. We then find the maximal number of nodes from N that can have kernel size of 2, and the rest of the nodes will have kernel size of 1. Eq. 2 shows our kernel size and stride size calculation and Figure. 1 illustrates our pseudo-alignment heuristic.

$$\begin{cases} S = \lceil \text{avg}(1, \lfloor \frac{M}{N-1} \rfloor) \rceil, \\ W = M - (N - 1) * S \\ S = 2, W = 2 \end{cases} \quad \begin{cases} \text{if } N \leq \frac{M}{2} \\ \text{otherwise} \end{cases} \quad (2)$$

B Model Efficiency

Number of Parameters. We compare the parameter efficiency of our model against the SOTA model, the Multimodal Transformer (MulT) (Tsai et al. 2019a). We first look at the total number of parameters used by the two models. Table 3 illustrates that our model uses 0.14 million parameters, only 6.3% of those in MulT, which has 2.24 million parameters, and yet still achieves state-of-the-art performance. We attribute this result to the effective early fusion of multiple (more than 2) modalities using the MTGAT component. In MulT, trimodal fusion happens at a very late stage of the architecture, since each cross-modal Transformer can only model bi-modal interactions. This late fusion regime requires earlier layers to preserve more original information, and thus resulting in a need for more model parameters.

Convergence. Figure 2 gives a comparison between the convergence speed of our model and MulT. Both models

Hyperparameter	CMU-MOSI	IEMOCAP
Batch Size	64	64
Initial Learning Rate	1e-3	1e-3
Optimizer	Adam	Adam
Number of MTGAT Layers	6	2
Number of Attention Heads	4	8
Node Embedding Dimension	64	64
Edge Pruning Keep Percentage	80%	80%
Total Epochs	20	35

Table 1: Hyperparameter settings on CMU-MOSI and IEMOCAP benchmarks.

Model \ Dataset	CMU-MOSI	IEMOCAP
MuT	27.2 \pm 2.33	56.0 \pm 4.59
MTGAT (ours)	24.4\pm0.95	44.4\pm0.55

Table 2: Training time per epoch (in seconds) comparison. Run time is averaged over 5 training epochs, with the subscript denoting standard deviation. Both models use batch_size=32, num_layers=6 and are run on the same machine with a single GPU of Nvidia GTX 1080 Ti. Both benchmarks used are the unaligned version.

are trained with batch_size=32 and lr=1e-3, with the default (best) hyperparameters used for both models. We use the unalignd CMU-MOSI for this study. We observe MTGAT converges much faster at epoch 12, comparing with MuT at epoch 17. In addition, we see that our validation MAE curve on the unaligned MOSI validation set goes consistently below MuT’s curve. This faster convergence performance could be explained by the small amount of parameters MTGAT uses - MTGAT has a much smaller parameter search space for the optimizer, resulting in faster training and earlier convergence.

Training time. We also compare how fast our model runs against MuT. Specifically, under the same condition, we calculate the time it takes for each model to run training for 1 epoch. Table 2 shows the details. We can see that our model runs significantly faster than MuT on both benchmarks, which can be attributed to our light-weight model design (as shown in Table 3). Meanwhile, our edge pruning also reduces the number of computation by throwing away edges that are deemed less important by the model, thus improving the run-time of our model.

Overall Efficiency. From the perspective of training time, number of parameters used, and convergence analysis, it is clear that our model is capable of achieving better results while using much smaller amount of computational resources

Model	# Parameters
MuT (previous SOTA)	2,240,921
MTGAT (ours)	142,363

Table 3: Number of model parameters comparison.

than the previous state of the art.

C Word-Aligned and Unaligned Data

We provide more details regarding the word-aligned and unalignd data sequences. In the word-aligned version, video and audio features are average-pooled based on word boundaries (extracted using P2FA (Yuan and Liberman 2008)) resulting in an equal sequence lengths of 50 for all three modalities. In the unaligned version, original audio and video features are used, resulting in a variable sequence lengths. For both datasets, the multimodal features are extracted from the textual (GloVe word embeddings (Pennington, Socher, and Manning 2014)), visual (Facet (iMotions 2017)), and acoustic (COVAREP (Degottex et al. 2014)) data modalities.

D Hyperparameters

We elaborate on the technical details including hyperparameter settings in Table 1. We conduct a basic grid search to find good hyperparameters such as initial learning rate, number of MTGAT layers etc. We use Adam as our optimizer and decays the learning rate by half whenever the validation loss plateaus. Notice that we are using a design that roughly yields a model with a similar structure as in previous works such as MuT. Nevertheless, we still manage to use far less number of parameters during optimization. We use one NVIDIA GTX 1080 Ti for training and evaluation. In addition, the model and hyperparameters we use for ablation study are the same as the ones used for the main experiment, both of which are conducted on CMU-MOSI.

E Number of Parameters Comparison

For a fair comparison on number of parameters between MTGAT and MulT, we use the same number of layers and attention heads for both models (i.e. 6 layers of MulT with 4 attention heads). A detailed comparison is shown in Table 3.